REPORT DOCUMENTATION PAGE

OMB No. 0704-0188

1. AGENCY USE ONLY (Leave blank)	2. REPORT DATE	3. REPORT TYPE AND DATES COVERED
	8/Aug/96	Interim

4. TITLE AND SUBTITLE
Boron Oxide Oligamer Collision-Induced Dissociation Thermochemistry, Structure, and Implications for boron Combustion

5. FUNDING NUMBERS
G N00014-95-10696

6. AUTHOR(S)
D. Peiris, A. Lapicki, and S.L. Anderson

7. PERFORMING ORGANIZATION NAME(S) AND ADDRESS(ES)
Department of Chemsitry
Universiy of Utah
Salt Lake City, UT 84112

8. PERFORMING ORGANIZATION REPORT NUMBER
UUIL -001

9. SPONSORING/MONITORING AGENCY NAME(S) AND ADDRESS(ES)
Office of Naval Research, Code 333
Mechanics and Energy Conversion Division
800 N. Quincy St
Arlington, VA 22217

10. SPONSORING/MONITORING AGENCY REPORT NUMBER

11. SUPPLEMENTARY NOTES

12a. DISTRIBUTION/AVAILABILITY STATEMENT

12b. DISTRIBUTION CODE

13. ABSTRACT *(Maximum 200 words)*

This report presents a collision-induced dissociation (CID) study of small boron oxide cations, $B_nO_m^+$, motivated by a need for more accurate and reliable structural and thermodynamic information on both neutral and ionic boron oxides. This work compliments ongoing *ab initio* calculations by Page and co-workers, and provides many points of comparison between experiment and theory. In addition, the results of our CID study are important in interpretation of boron oxide cluster chemistry work in our lab.

14. SUBJECT TERMS
CID Boron Oxide Combustion

15. NUMBER OF PAGES
23

16. PRICE CODE

17. SECURITY CLASSIFICATION OF REPORT	18. SECURITY CLASSIFICATION OF THIS PAGE	19. SECURITY CLASSIFICATION OF ABSTRACT	20. LIMITATION OF ABST
none	none	none	

Boron Oxide Oligamer Collision-Induced Dissociation: Thermochemistry, Structure, and Implications for Boron Combustion

Dilrukshi Peiris, Adam Łapicki, and Scott L. Anderson

Chemistry Department, Univeristy of Utah, Salt Lake City, UT 84112

I. Introduction

This report presents a collision-induced dissociation (CID) study of small boron oxide cations, $B_nO_m^+$, motivated by a need for more accurate and reliable structural and thermodynamic information on both neutral and ionic boron oxides. This work compliments ongoing *ab initio* calculations by Page and co-workers, and provides many points of comparison between experiment and theory. In addition, the results of our CID study are important in interpretation of boron oxide cluster chemistry work in our lab.

In combustion of boron or boron rich fuels and propellants, boron oxide chemistry plays two important roles. Boron particles are naturally coated with a passivating layer of the oxide, which may be at least partly converted to hydroxide (i.e. boric acid) depending on humidity and temperature. As the particles heat up in a combustion environment, the oxide layer retards boron ignition until it is removed. This occurs by evaporation at high temperatures, but the potential exists to accelerate ignition by chemical volatilization at lower temperatures. Boron oxide properties are also important in achieving energy release in the post-oxidation chemistry. In particular, full energy release only occurs if the gaseous $B_nO_mH_l$ oxidation products condense to thermodynamically stable products such as $B_2O_3(\ell)$, rather than remaining as $(B_nO_mH_l)_k$ oligomers. Clearly, the chemistry and thermodynamics of small $B_nO_mH_l$ species are important in this process.

A promising strategy to enhance boron combustion is to fluorinate the hydrocarbon components of a boron-containing propellant. Decomposition of the hydrocarbon releases HF, that can attack the boron or boron oxide particle surfaces. Since boron has a high affinity for fluorine, and F is isoelectronic with OH, fluorine will tend to displace OH or O from oxides, forming stable $B_nO_mH_lF_k$ species. Since fluorine compounds of boron are more volatile than oxides or hydroxides, HF attack should tend to volatilize the oxide layer. Indeed FBO is observed as the major product of HF attack on small boron oxide cluster ions (1), in accord with modeling predictions based on thermodynamic considerations (2,3).

In the course of the HF/boron oxide cluster study, we found substantial uncertainties in the thermodynamics reported for small $B_nO_mH_lF_k$ compounds. Much of the thermochemistry is based on very low-level *ab initio* or semi-empirical quantum chemistry calculations, that are not expected to be very reliable. Recent and on-going high quality *ab initio* calculations by Linder and Page (4,6) and Soto (5) are improving the situation dramatically, however, there is little experimental data available to test the accuracy of the calculations. The results reported here largely validate the accuracy of the Linder and Page calculations, while their results provide considerable insight into our experiments.

One major puzzle remains. In the course of our HF/$B_nO_m^+$ study we observed a reaction producing FBOH. From the energy dependence of the cross section for this reaction, it clearly is exothermic and based on estimates of the thermodynamics for $B_nO_m^+$, we predicted that FBOH should have a ΔH_f no higher than -194 kcal/mole. This is 80 kcal/mole more stable than predicted by the calculations of Page and co-workers (6) and Soto (5), and this discrepancy is far outside the usual uncertainties expected for calculations of that quality. Our ΔH_f was based in part on

estimates for the thermochemistry of the larger $B_nO_m^+$ species, and this seemed to be a likely source of the disagreement. One motivation for the present CID study was, therefore, to determine the stabilities of these species directly. Despite overall good agreement between our experiments and the calculations, this particular controversy has not been resolved.

II. Experimental Method

Apparatus. The cluster beam instrument and operating procedures used for these experiments has been described in detail elsewhere (1,7,8). Briefly, boron oxide cluster ions are generated by 12 keV argon atom bombardment (9) of a film of vitreous B_2O_3 maintained near its melting point. The nascent $B_xO_y^+$ cluster ions are collected by a radio-frequency (rf) octapole ion guide and cooled to near room temperature by storage in a labyrinthine rf trap containing ~0.01 Torr of helium buffer gas. The reactant cluster ion size and composition is selected using a quadrupole mass filter and then the beam is injected into another octapole ion guide system where scattering is carried out. The octapole sets the collision energy and guides the ions through a collision cell filled with either xenon or argon to a typical pressure of 1×10^{-5} Torr. For these experiments we need single collision conditions, and this was checked by measuring cross sections over a range of xenon/argon pressures. Fragment ions and the remaining parent ions are collected by the octapole, mass analyzed by a second quadrupole mass spectrometer, and counted.

Sample Preparation. Isotopically purified (94.11 At.% of ^{10}B) boron oxide (B_2O_3) powder (Eagle-Pitcher) was sprinkled on a stainless steel substrate, then heated in a furnace at 650°C for about four hours in oxygen environment to produce a vitreous film. Because boron oxide is found to be highly hygroscopic, the sample is maintained a 350-450°C in the high vacuum cluster source chamber.

III. Results

Reactant Beam Kinetic Energy Distribution. Accurate CID threshold determinations require a narrow and well defined kinetic energy distribution for the primary beam. This is measured by retarding potential analysis and controlled by fine adjustments of the focussing lens system. A typical retarding potential curve is shown in Figure 1 correspond to a beam energy width of ~ 0.240 eV. The beam energy distribution is obtained by fitting this retarding curves to a 3 parameter asymmetric Lorentzian function:

$$F(x) = \frac{A}{\{1+[(x-E_0)/b]^2\}\exp(x-E_0)^c}$$

E_0 represents the shift in average beam energy relative to the nominal LAB KE of the ions, the energy width is determined by b, and c is allows fitting the asymmetry of the distribution (usually quite small).

Reaction Cross Sections and Branching Patterns. Absolute fragmentation cross sections were measured for all observable $B_nO_m^+$ ($n<4$, $m<5$) parent ions at center-of-mass collision energies ranging from 0.8 to 10 eV. Cross sections are shown for all significant fragmentation channels in Figures 2a through 2g. Fragmentation in collision with both argon and xenon was studied and the best results are presented. Xenon generally seems to be a more efficient target gas, however, argon was found to be superior for several of the smallest cluster ions. To summarize trends with changing cluster size, Figure 3 reports the total fragmentation cross section and the fragment patterns at a fixed collision energy of 9.5 eV -- well above the threshold range for all cluster sizes.

Extracting CID Thresholds. To obtain quantitative dissociation thresholds from the

experimental data we need to correct for the collision energy spread resulting from the beam energy distribution and the thermal motion of the target gas. This was done by a standard convolution and fitting approach that has been described in detail previously (10). Briefly, the cross sections in the threshold region were modeled using an assumed "true" cross section functional form that has been widely used in the scattering community:

$$\sigma(E_{avail}) = \frac{A\,(E_{avail} - E_0)^n}{E_{avail}}$$

where A is a normalization factor, E_0 is the dissociation threshold, n is an adjustable parameter that varies the curvature of the function, physically related to the energy transfer efficiency, and E_{avail} is the total energy available to drive fragmentation.

This trial function is convoluted (through a Monte Carlo simulation) with the kinetic energy distribution of the primary cluster ions, the translational energy distribution of the target gas, and the distribution of vibrational and rotational energy of cluster ions. The vibrational energy has been calculated assuming that the clusters are at 400 K, using vibrational frequencies from *ab initio* calculations (6). The parameters n and E_0 are optimized until a best fit is obtained. Fitting was attempted only for the lowest energy fragmentation channel for each reactant cluster ion. In principle, additional thermochemical information can be extracted from the higher energy dissociation channels, however, this analysis is complicated by a difficult-to-estimate kinetic shift factor.

The best fits for the lowest energy fragmentation channels are shown in Figures 2a - 2g. The curves labeled "Best fit" are best free fits to the data, and the extracted E_0 values are the experimental estimates for dissociation energies. We also plot "Fit to Theory" curves. These are

fits based on E_0 values calculated by Linder and Page (6) with only the n parameter adjusted in an attempt to fit the data. These are plotted to show the cases for which the experiment and theory are or are not in agreement. The fit thresholds (E_0) and n parameters for the lowest-energy dissociation channel of each cluster for both types of fittings are given in Table I, along with the calculated dissociation thresholds. The cluster stability, represented by the lowest-energy dissociation thresholds, is plotted as a function of size in Figure 3 (scatter plot, right-hand scale). In addition, stability is plotted as a function of boron-to-oxygen ratio in Figure 4.

IV. Discussion

Fragmentation Branching Ratios. In fragmentation reactions, two factors can contol the branching between different possible fragment channels. In some cases, one might expect that the geometrical struture of the parent cluster ion would be reflected in the fragments, i.e. that fragmentation might occur by simple bond rupture, without rearrangement. This is particularly likely in high energy CID, where the fragmentation time scale is short. In low energy CID, such as our near-threshold work, the fragmentation time scale is long enough that rearrangement can occur prior to, or during, decomposition. In this case, the fragment branching is influenced strongly by the thermochemistry of the possible products, with the most stable products dominating.

Based on the available thermochemistry in the literature (1,4,5,11) and the on-going *ab initio* calculations by Linder and Page, it appears that product thermochemistry is the dominant factor for all but one of the boron oxide cluster ions we have examined. For BO^+, B_2O^+, $B_2O_2^+$, and $B_3O_3^+$ -- all clusters where the number of B atoms is equal to or greater than the number of O atoms in the parent cluster, the dominant fragmentation pathway is loss of B^+. This appears to

reflect two factors: the low ionization potential of the boron atom, and the relatively high stability of fragments with B_nO_{n+1} stoichiometry.

For the $B_2O_3^+$ parent cluster, the only important fragmentation channel is loss of O, yielding $B_2O_2^+$. Dissociation to $BO^+ + BO_2$, only 0.5 eV higher in energy, accounts for only a few percent of the products, even at energies well above threshold. $B_3O_4^+$ which also prefers to decompose to $B_2O_2^+$ (+ BO_2), produces a substantial branching to the nearly isoenergetic fragment pairs $B_2O_3^+ + BO$ and $BO^+ + B_2O_3$ that lie ~0.3 higher in energy.

The one exception to control by fragment thermochemistry is BO_2^+. The dominant decomposition channel is to $BO^+ + O$, even though the $B^+ + O_2$ channel is ~1.6 eV lower in energy. This presumably reflects either a barrier or dynamical bottleneck that inhibits passage from the parent OBO structure to a transition where O_2 elimination can occur. Some B^+ is observed with approximately the same appearance energy as the main BO^+ channel. The competition between these channels makes analysis of the $BO^+ + O$ threshold somewhat ambiguous.

Given that thermochemistry appears to control the fragment branching, some energetic insight can be inferred directly from the branching patterns. In several cases we observe pairs of channels that differ only in which fragment carries the charge:

$$M^+ \rightarrow A^+ + B$$
$$\rightarrow A + B^+.$$

As the fragments separate, we expect that the charge will largely end up on the fragment with the lower ionization potential (IP). If the IPs are similar both pairs of channels will be observed, but if the difference is large, we expect significant signal only for the lower energy fragment pair.

Based on this assumption, we can infer relationships between IPs for a number of B_nO_m species and these are summarized in Table I. In many cases these are not surprising and agree with literature thermochemistry. In others, the literature values are inconsistent with our results or no literature values are available. The on-going calculations of Linder and Page appear to be consistent with our findings in all cases.

One notable example is B_2O_3. The existing literature gives an IP for B_2O_3 of 13.56 eV (11). Our fragmentation branching for $B_3O_4^+$ indicates that $IP(B_2O_3) < IP(BO)$, given as 13.0 eV in the literature. Linder and Page have calculated IP(BO) = 13.1 eV and $IP(B_2O_3)$ = 12.9 eV, consistent with our findings.

Fragmentation Threshold Energies and Relation to Theory.

These CID experiments show that BO_2^+ is the most stable and B_2O^+ the least stable cluster studied. The stability of the boron oxide clusters plotted as a function of the cluster size (Figure 3) exhibits an oscillating pattern typical for most of size dependence cluster studies (8,10). Furthermore, the stability clearly is strongly anticorrelated to the B:O ratio in the cluster (Figure 4). As expected maximum stability is promoted by increasing the possibility for BO bonding.

Table II gives the best fit dissociation threshold extracted as discussed above, along with the associated value of the "n" parameter. Also given are the dissociation energies calculated by Linder and Page. Note that the experimental uncertainties are abnormally large for these oxide cluster ions. This results from the fact that the fragmentation cross sections are unusually small (at maximum, only a few percent of the collision cross sections) and rise rather slowly from threshold. This suggests that collisional energy transfer is particularly inefficient for these

clusters. The result is a larger-than-usual degree of arbitrariness in picking the best fit in the near-threshold energy range because the signal rise very slowly out of the background. To give a clearer idea of which experimental dissociation threshold (E_0) values agree/disagree with the calculated dissociation energies, figures 2a-2g plot the best fits obtainable using the calculated E_0 values.

For BO^+ there is an apparent discrepancy between the experimental and calculated E_0, however, as figure 2a shows, the "best" and "theory" fits are rather similar. BO^+ has an especially small CID cross section, and the data are not good enough to justify concluding that the discrepancy is real.

For B_2O^+ and some of the larger clusters there is an additional complication. Linder and Page calculate that the BOB^+ isomer is most stable, but that cyclic and BBO^+ isomers lie only 0.2 eV and 0.3 eV higher in energy. For this situation, it is not unlikely that our cluster beam contains some admixture of these higher energy isomers, which would give a threshold of ~1.6 eV, in good agreement with the experiment. Because CID is inherently sensitive to the least stable species present, only a few percent of a high energy isomer is needed to skew the threshold. This is NOT the case for reactive scattering, where usually we are looking a far more efficient process than CID.

This example raises the issue of the isomer distributions found in our cluster ion beams. Our cluster ions are produced by laser ablation, or in this case, particle sputtering. Both methods produce a distribution of cluster sizes with very high internal temperatures. These hot cluster ions initially cool by evaporation, then are actively cooled by collisional quenching in helium buffer gas over a ~1 second period. Based on previous tests, we are pretty confident that the clusters have

internal temperatures near room temperature. As the clusters cool down, we normally would expect that nearly all the clusters will anneal to the lowest energy isomer, since the density of states is highest in the deepest well. Indeed, in our previous studies of boron and carbon cluster ions, the evidence (agreement with theory, fragment distributions, and reactivity) indicates that with the exception of a few particular carbon clusters, only the most stable isomer is found. There are two cases where a substantial concentration of a higher energy isomer may be present. In the case of C_{7-9}, the linear and cyclic isomers are nearly isoenergetic, so that densities of states for each form are comparable.

The other likely case is if the activation barriers separating the potential minima corresponding to the two isomers are large compared to the energy difference between them. In this case the barrier crossing rate will decrease rapidly early in the cooling process, thus freezing in an isomer distribution corresponding to a temperature far above the final cluster temperature. For some of these boron oxide clusters, this may indeed be the case. The clusters are generally singly connected (unlike boron for example) so that the bond order reduction in fragmentation is similar to that in the type of transition state that seems likely for the isomerization. This issue is being examined by Linder and Page, who are calculating isomerization activation barriers for some of the clusters where multiple isomers seem likely. If this does turn out to be a problem in the experiments, we can attempt to remove the higher energy isomers by titrating them out during the cooling process using a suitable reactant --possibly water. This approach has been used successfully for carbon cluster ions.

For BO_2^+ (unlikely to have any stable isomers other than OBO^+) our best fit E_0 is somewhat lower than the calculated E_0, but as in the BO^+ case, this cluster has a small

fragmentation cross section and the experimental uncertainty is therefore high.

$B_2O_2^+$ is really the first cluster where there clearly is a difference between the data and calculation. The experimental signal/noise is better here, and the "fit to theory" does not adequately reproduce the threshold behavior. It is possible that this reflects a problem in the calculations, however, $B_2O_2^+$ is another case where a low lying isomer might skew the experiments. Linder and Page predict that there is a cyclic isomer lying ~0.8 eV above the most stable $OBOB^+$ geometry. This would give a threshold of 3.3 eV, consistent with the measured E_0.

$B_2O_3^+$ is a case where isomers other than the ground state $OBOBO^+$ are not expected to be low enough lying to be significantly populated. For this cluster the experimental and calculated E_0 values are in nearly perfect agreement.

$B_3O_3^+$ is another case where it is not possible to fit the experimental data with the E_0 value calculated by Linder and Page. The experimental E_0 is over 1 eV lower than the calculation. As with all the oxides with B:O ratio equal to or greater than unity, several low lying isomers are likely. The calculations find the $OBBOBO^+$ structure to be most stable, but $OBOBOB^+$ and a structure with a 4-membered ring are both calculated to be within ~1 eV of the ground state. A small admixture of one or both of these might explain the near-threshold discrepancy shown in figure 2f.

For $B_3O_4^+$ both intuition and the Linder-Page calculations suggest a $OBOBOBO^+$ structure. Calculations are on-going, but to date no other low-lying isomers have been found. Nonetheless there is a substantial discrepancy between the experimental E_0 (4.25 eV) and that derived from the calculations (6.4 eV). At this point, the origin of the disagreement is not clear.

Implications for FBOH thermochemistry. Another unresolved discrepancy is the heat of formation of FBOH. In our studies of boron oxide cluster ion reactions with HF, one of the major product channels observed was elimination of FBOH:

$$B_nO_m^+ + HF \rightarrow B_{n-1}O_{m-1}^+ + FBOH$$

$$\rightarrow B_{n-1}O_{m-1} + FBOH^+$$

Production of neutral FBOH is inferred from the $B_{n-1}O_{m-1}^+$ product, for which FBOH is the lowest energy neutral partner. In reaction with $B_3O_4^+$, both these channels are observed with nearly equal intensities and with substantial cross sections at low collision energies, indicating that both are exothermic. The observation that the reaction producing $B_{n-1}O_{m-1}^+$ (+ FBOH) is exoergic allows us to put an upper limit on ΔH_f(FBOH). Taking Linder and Page's calculated ΔH_f values for $B_3O_4^+$ (- 44.2 kcal/mole) and $B_2O_3^+$ (100.8 kcal/mole), this requires that ΔH_f(FBOH) < 210 kcal/mole. This compares poorly with the *ab initio* ΔH_f(FBOH) = ~-113 kcal/mole calculated by Soto (5) and Page (4). Our CID results find $B_3O_4^+$ to be ~49 kcal/mole less stable than calculated by Linder and Page. If we use this to estimate $\Delta H_f(B_3O_4^+)$ = ~5 kcal/mole, this still requires that ΔH_f(FBOH) < ~160 kcal/mole. In either case, the discrepancy with the *ab initio* value is way outside the range of errors normally associated with those calculations.

The idea that FBOH is considerably more stable than the *ab initio* calculations suggest is supported by the observation that the ($B_{n-1}O_{m-1}^+$ + FBOH) and ($B_{n-1}O_{m-1}$ + $FBOH^+$) product channels have nearly equal intensity for reaction of $B_3O_4^+$ with HF. This suggests that IP(FBOH) ≈ IP(B_2O_3) = 12.9 eV (6). The difference between *ab initio* ΔH_f values for FBOH and for $FBOH^+$ (the latter being consistent with our results) gives IP(FBOH) = ~7.5 eV. If this were

correct, it seems unlikely that we would see significant signal for the $B_{n-1}O_{m-1}^+$ + FBOH channel because the charge should overwhelmingly migrate to FBOH as the products separate.

Conclusions

Our CID results help clarify some of the confusion in the thermochemical literature for small boron oxide oligamers. The results are largely consistent with the new *ab initio* calculations of Linder and Page, though there are some unresolved issues regarding isomer distributions that make direct comparisons ambiguous for some cluster sizes. Significant (and related) discrepancies between theory and experiment exist for $B_3O_4^+$ and for FBOH. As the calculations are completed for $B_3O_4^+$, it may be possible to resolve these disagreements.

Acknowledgements

We are grateful to Doug Linder and Michael Page for providing results of their *ab initio* calculations prior to publication. This work was supported by the Office of Naval Research, Mechanics and Energy Conversion Division under grant N00014-95-10696.

References

1. Smolanoff, J.; Lapicki, A.; Kline, N.; Anderson, S. L. *J. Phys. Chem.* **1995,** *99,* 16276.

2. Brown, R. C.; Kolb, C. E.; Rabitz, H.; Cho, S. Y.; Yetter, R. A.; Dryer, F. L. *Int. J. Chem. Kinetics* **1991,** *23,* 957.

3. Yetter, R. A.; Rabitz, H.; Dryer, F. L.; Brown, R. C.; Kolb, C. E. *Combust.and Flame* **1991,** *83,* 43.

4. Page, M. *J. Phys. Chem.* **1989,** *93,* 3639; Page, M., private communication.

5. Soto, M. *J. Phys. Chem.* **1995,**

6. Page, M.; Linder, D., private communication.

7. Hanley, L.; Ruatta, S. A.; Anderson, S. L. *J. Chem. Phys.* **1987,** *87,* 260.

8. Hanley, L.; Whitten, J. L.; Anderson, S. L. *J. Phys. Chem.* **1988,** *92,* 5803.

9. Alexander, A. J.; Hogg, A. M. *Int. J. Mass Spectrom. Ion Processes* **1986,** *69,* 297.

10. Sowa-Resat, M. B.; Hintz, P. A.; Anderson, S. L. J. *Phys. Chem.* **1995,** *99,* 10736 and references therein.

11. Lias, S. G.; Bartmess, J. E.; Liebmann, J. F.; Holmes, J. L.; Levin, R. D.; *J. Phys. Chem. Ref. Data* **1988,** *17,* Suppl. 1.

12. Nguyen, M. T.; Vanquickenborne, L. G.; Sana, M.; Leroy, G. *J. Phys. Chem.* **1993,** *97,* 5224.

Table I. Comparisons of the Ionization Potentials of Boron oxide Cluster Ions.

parent oxide cluster	IP relations inferred	literature IP relations[a]	Linder and Page IP relations
B_2O^+	IP(BO) >> IP(B)	IP(BO) = 13.0eV IP(B) = 8.298eV consistent	IP(BO) = 13.1eV IP(B) = 8.30eV
$B_2O_2^+$	$IP(BO_2)$ > IP(B)	$IP(BO_2)$ = 13.5eV consistent	$IP(BO_2)$ = 13.66eV
$B_2O_3^+$	IP(BO)≈ $IP(BO_2)$	consistent	IP(BO) ≈ $IP(BO_2)$
$B_3O_3^+$	$IP(B_2O_3)$ >> IP(B) IP(BO) > $IP(B_2O_2)$	$IP(B_2O_3)$ = 13.56eV consistent $IP(B_2O_2)$ = 13.58eV inconsistent	$IP(B_2O_3)$ = 13.15eV $IP(B_2O_2)$ = 10.37eV
$B_3O_4^+$	IP(BO) > $IP(B_2O_3)$ $IP(BO_2)$ > $IP(B_2O_2)$	inconsistent inconsistent	

[a] Lias, S. G., Bartmess, J. E., Liebman, J. F., Holmes, J. L., Levin, R. D., Mallard, W. G. *J. Phys. Chem. Ref. Data,* **1988,** vol. 17, Suppl.1.

Table II. Best Fit parameters (n) and Best Fit Dissociation Energy Thresholds (E_0) of Boron Oxide Cluster Ions.

dissociation channel	best fit		[a]fit to theory	
	n	**E_0**	**n**	**E_0**
$BO^+ \rightarrow B^+ + O$	1.90	2.75 ± 0.6	1.35	3.60
$B_2O^+ \rightarrow B^+ + BO$	1.80	1.30 ± 0.5	1.40	1.90
$BO_2^+ \rightarrow BO^+ + O$	1.60	4.75 ± 0.6	1.05	5.60
$B_2O_2^+ \rightarrow B^+ + BO_2$	1.30	3.15 ± 0.2	1.05	4.10
$B_2O_3^+ \rightarrow B_2O_2^+ + O$	1.64	5.10 ± 0.2	1.70	5.09
$B_3O_3^+ \rightarrow B^+ + B_2O_3$	2.05	2.00 ± 0.2	1.05	3.2
$B_3O_4^+ \rightarrow B_2O_2^+ + BO_2$	2.10	4.25 ± 0.5	1.1	6.4

[a] E_0 values from reference 6.

Figure Captions

1. A typical retarding potential curve.

2. Cross sections for all significant fragmentation channels along with the best fits for the lowest energy dissociation pathways of boron oxide cluster cations.

3. The total fragmentaion cross section and the fragmentation patterns at a fixed collision energy of 10 eV. The cluster stability as a function of size is shown by the scatter plot (right-hand scale).

4. The cluster cations's stability as a function of boron-to-oxygen ratio.

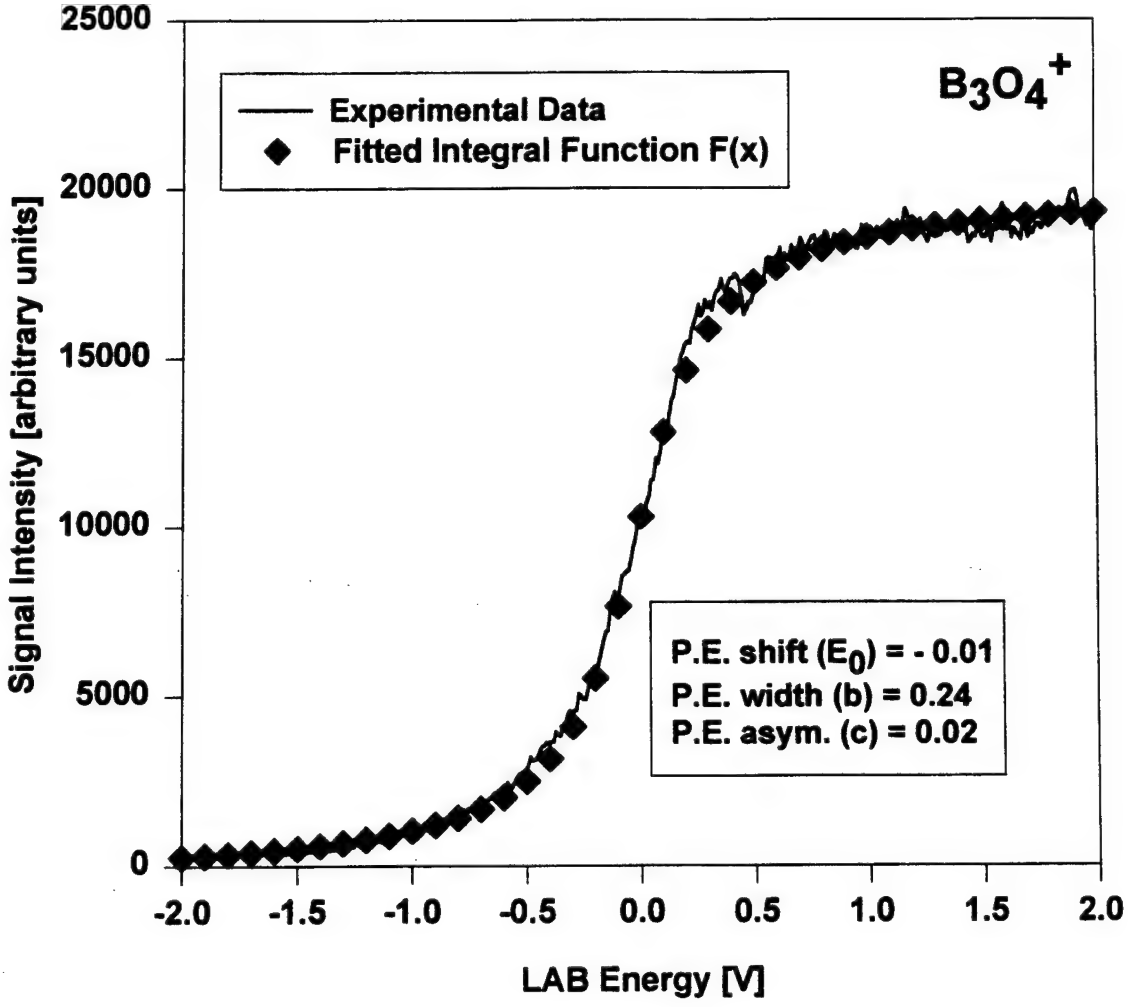
25000
20000
15000
10000
5000
0
Signal Intensity [arbitrary units]
-2.0
-1.5
-1.0
-0.5
0.0
0.5
1.0
1.5
2.0
LAB Energy [V]
Experimental Data
Fitted Integral Function F(x)
$B_3O_4^+$
P.E. shift (E_0) = - 0.01
P.E. width (b) = 0.24
P.E. asym. (c) = 0.02

Fig 1

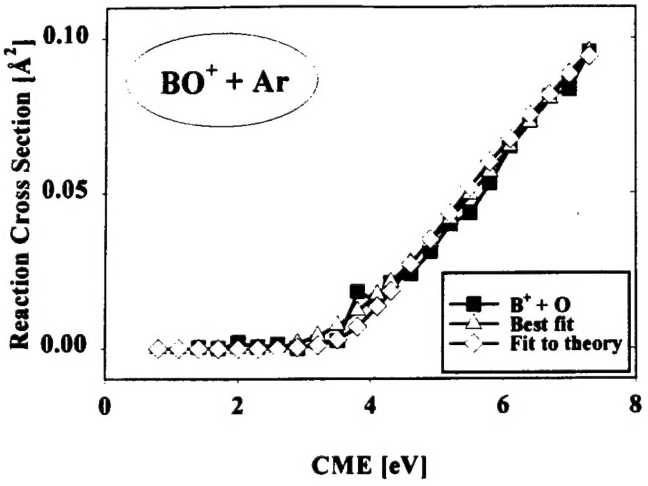
$BO^+ + Ar$
Reaction Cross Section [Å^2]
0.10
0.05
0.00
0
2
4
6
8
CME [eV]
$B^+ + O$
Best fit
Fit to theory

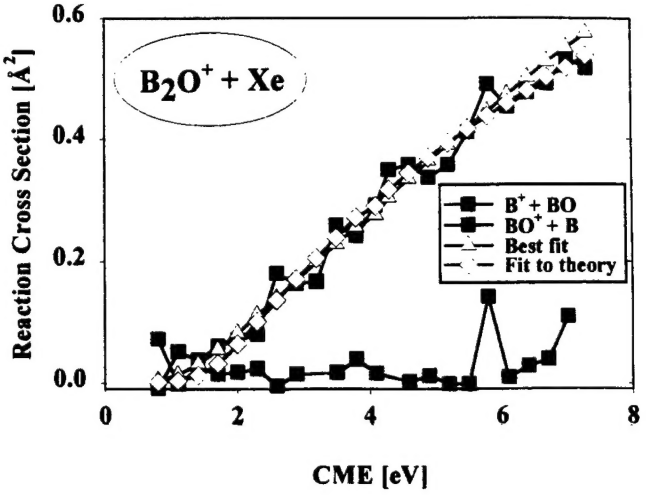
$B_2O^+ + Xe$
Reaction Cross Section [Å^2]
0.6
0.4
0.2
0.0
0
2
4
6
8
CME [eV]
$B^+ + BO$
$BO^+ + B$
Best fit
Fit to theory

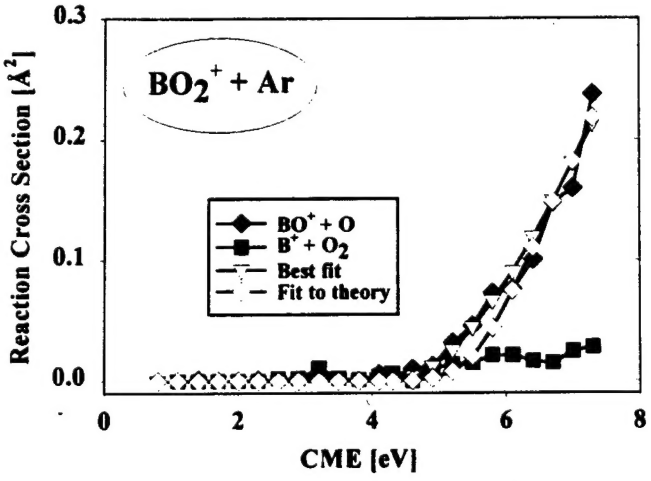
$BO_2^+ + Ar$
Reaction Cross Section [Å^2]
0.3
0.2
0.1
0.0
0
2
4
6
8
CME [eV]
$BO^+ + O$
$B^+ + O_2$
Best fit
Fit to theory

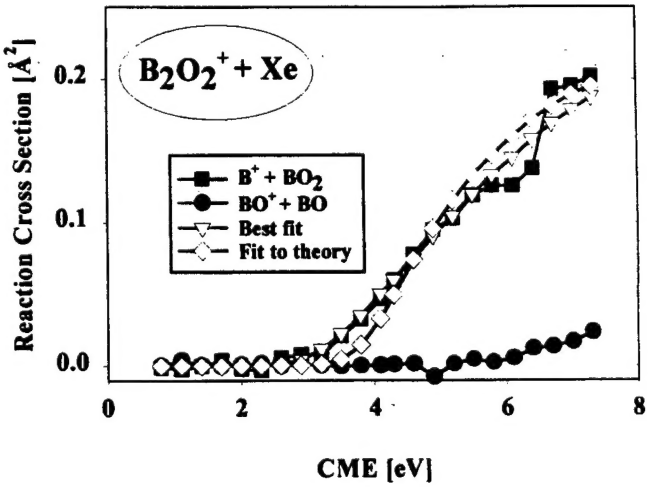
$B_2O_2^+ + Xe$
Reaction Cross Section [Å^2]
0.2
0.1
0.0
0
2
4
6
8
CME [eV]
$B^+ + BO_2$
$BO^+ + BO$
Best fit
Fit to theory

Fig 2 a-d

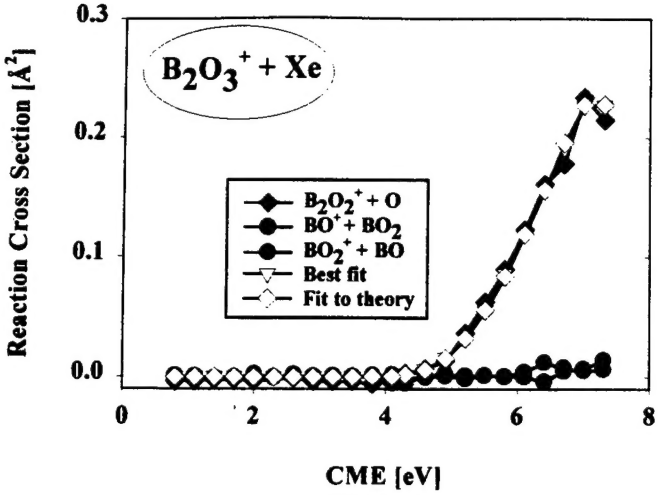
$B_2O_3^+ + Xe$
$B_2O_2^+ + O$
$BO^+ + BO_2$
$BO_2^+ + BO$
Best fit
Fit to theory
Reaction Cross Section [Å^2]
CME [eV]

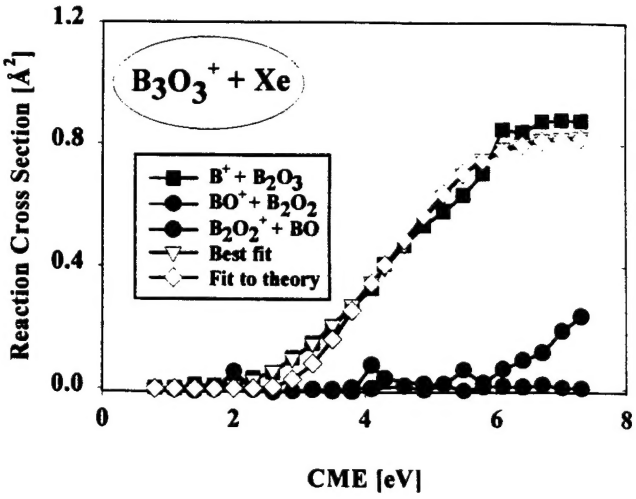
$B_3O_3^+ + Xe$
$B^+ + B_2O_3$
$BO^+ + B_2O_2$
$B_2O_2^+ + BO$
Best fit
Fit to theory
Reaction Cross Section [Å^2]
CME [eV]

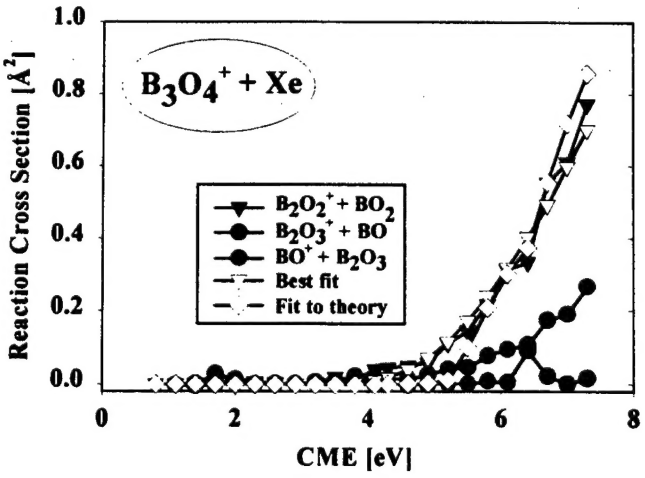
$B_3O_4^+ + Xe$
$B_2O_2^+ + BO_2$
$B_2O_3^+ + BO$
$BO^+ + B_2O_3$
Best fit
Fit to theory
Reaction Cross Section [Å^2]
CME [eV]

Fig 2 e-g

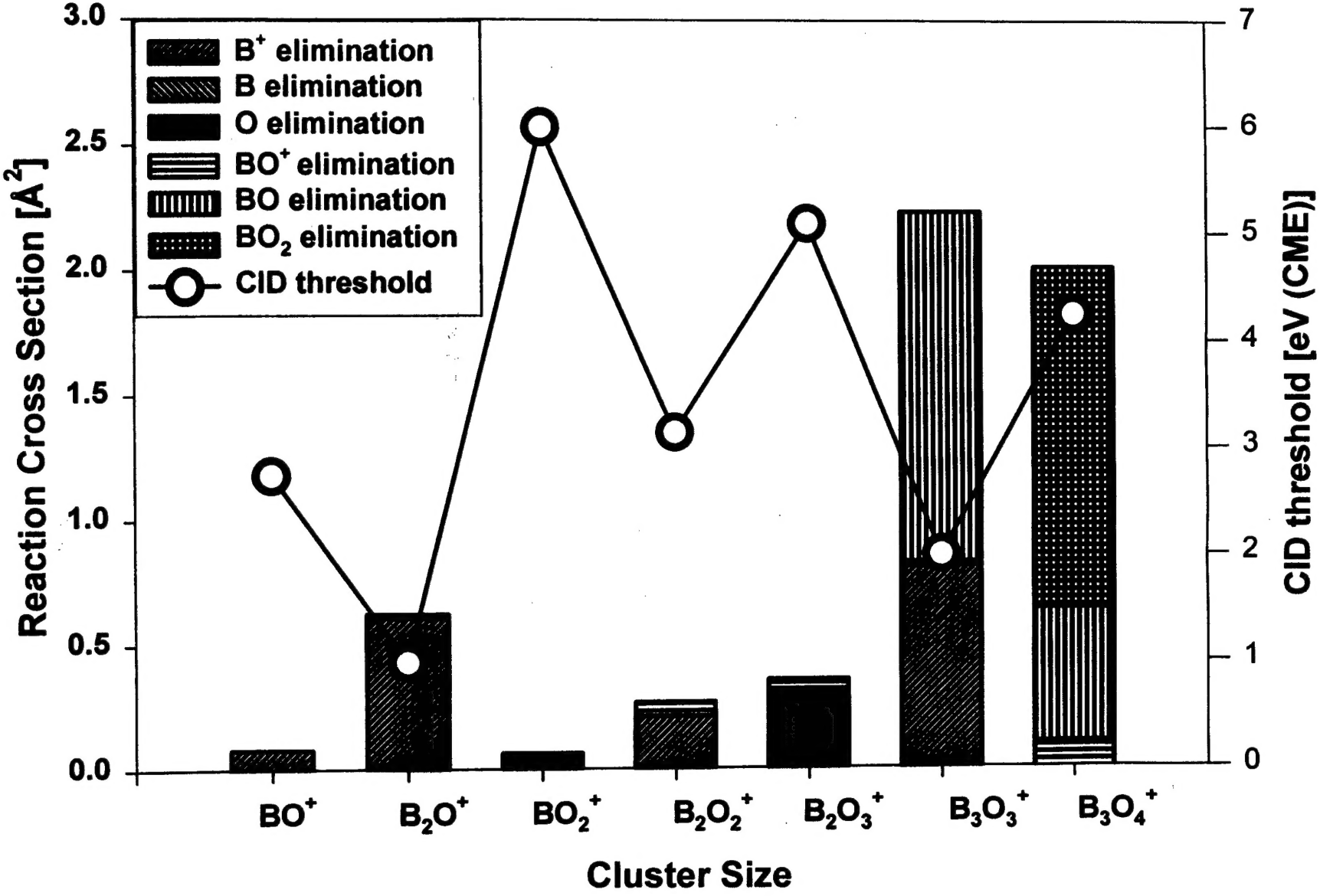
B+ elimination
B elimination
O elimination
BO+ elimination
BO elimination
BO2 elimination
CID threshold
Reaction Cross Section [A2]
CID threshold [eV (CME)]
3.0
2.5
2.0
1.5
1.0
0.5
0.0
7
6
5
4
3
2
1
0
BO+
B2O+
BO2+
B2O2+
B2O3+
B3O3+
B3O4+
Cluster Size

Fig. 3.

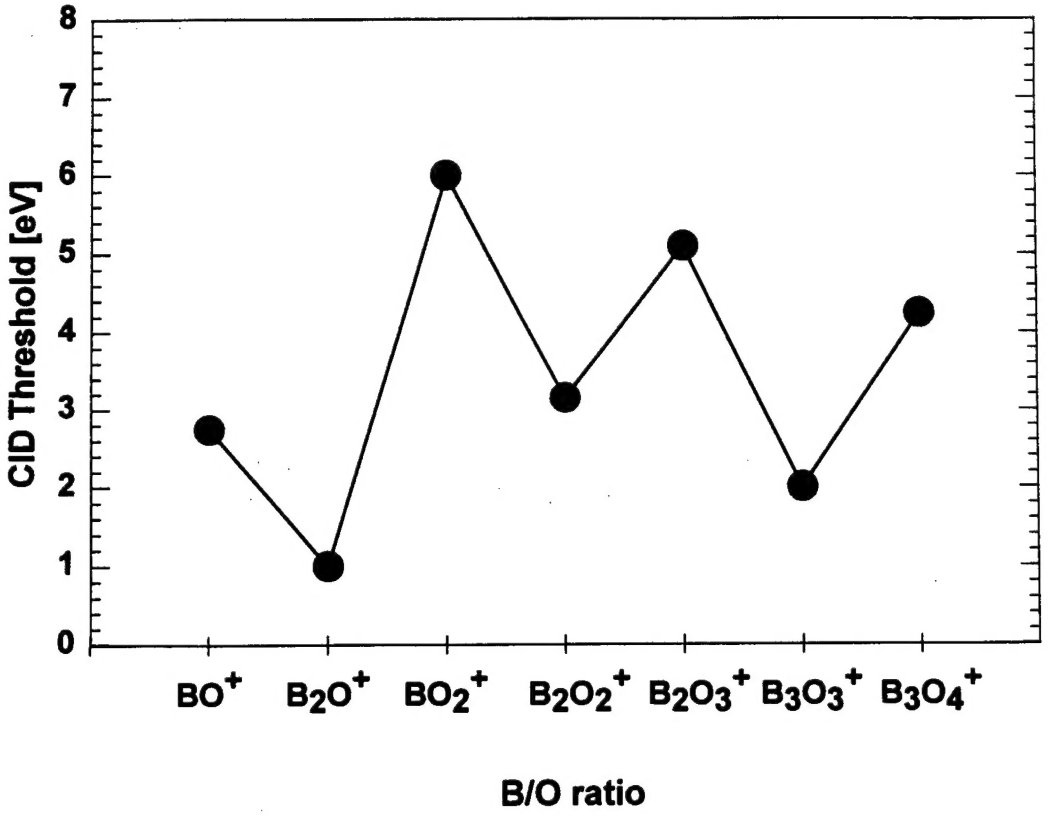
CID Threshold [eV]
0
1
2
3
4
5
6
7
8
BO+
B2O+
BO2+
B2O2+
B2O3+
B3O3+
B3O4+
B/O ratio

Fig 4